Journal of Petroleum Exploration and Production Technology
https://doi.org/10.1007/s13202-024-01763-1

ORIGINAL PAPER-PRODUCTION ENGINEERING

Optimization of CO_2 EOR and geological sequestration in high-water cut oil reservoirs

Jia Liu[1,2] · Fankun Meng[1,2] · Hui Zhao[1,2] · Yunfeng Xu[1,2] · Kai Wang[3] · Chenyang Shi[1,2] · Zifeng Chen[1,2]

Received: 3 March 2023 / Accepted: 27 January 2024

Abstract

In terms of the collaborative optimization of CO_2 flooding for Enhanced Oil Recovery (EOR) and CO_2 sequestration, previous studies have co-optimized both cumulative oil production and CO_2 sequestration by various algorithms. However, these solutions fail to optimize the CO_2 injection schemes for high-water cut oil reservoirs. This paper presents an optimization methodology for CO_2 flooding and sequestration in high-water cut oil reservoirs. The production optimization was carried out by adjusting the injection and production rate. To solve the proposed objective functions, the simultaneous perturbation stochastic approximation (SPSA) algorithm is applied in this paper, and the CMG-GEM module is utilized to simulate the reservoir production performance. A typical high-water cut reservoir in the Shengli oilfield was used to verify the feasibility of the presented methodology. In this paper, the production performance and net present value (*NPV*) for continuous gas injection under different water cuts were analyzed. The optimal timing of transforming from water flooding to gas displacement for the high-water cut reservoir was optimized. In addition, the optimal water–gas ratios for Water-Alternating-Gas (WAG) flooding were determined. The sensitivity of *NPV* to gas injection price and carbon subsidy was analyzed. The results show that when the gas price is 0.178 \$/m^3 and the carbon subsidy is 0.0169 \$/m^3, the optimal timing of transforming from water flooding to gas injection should be earlier than the time when the water cut is 0.82. Through the combination of *NPV*, cumulative oil production rate, and CO_2 sequestration volume for WAG flooding, the optimal WAG ratio should be 1:2. The presented method in this paper considers various economic indicators and can optimize CO_2 flooding and sequestration in high-water cut oil reservoirs efficiently, which can provide some guidance for the design of CO_2 flooding schemes in high-water cut oil reservoirs.

Keywords CO_2 sequestration · CO_2 EOR · High-water cut reservoir · Production optimization

List of symbols

BHP^{L}	Lower boundary of *BHP*, MPa
BHP^{U}	Upper boundary of *BHP*, MPa
C_t	Cash flow at the time *t*, \$
c_1	Perturbation quantity
f_w	Field water cut
k	Number of iterations
M	The sample size of the SPSA gradient
m_i	Logarithmic transformation model parameter
m_i^{L}	Lower boundary of the logarithmic transformation model parameter
m_i^{U}	Upper boundary of logarithmic transformation model parameter
n	Number of perforated wells
N_p	Cumulative oil production, m^3
$q^t_{g,p}$	Cumulative CO_2 volume separated from production wells, m^3
$q^t_{g,i}$	Cumulative volume of injected CO_2 during production time, m^3
$q_n^{\mathrm{L},t}$	Lower boundary of production rate, m^3/day
$q_n^{\mathrm{U},t}$	Upper boundary of production rate, m^3/day
q^t_o	Total oil production at time *t*, m^3
$q^t_{w,i}$	Total water injection rate at time *t*, m^3
$q^t_{w,p}$	Total water production rate at time *t*, m^3
r	Discount rate
$r_{g,i}$	Cost of injected gas, \$/m^3
r_o	Oil price, \$/m^3
$r_{w,i}$	Cost of water injection, \$/m^3

✉ Fankun Meng
mengfk09021021@163.com

1 Key Laboratory of Drilling and Production Engineering for Oil and Gas, Wuhan 430100, Hubei Province, China

2 School of Petroleum Engineering, Yangtze University, Wuhan 430100, China

3 Southern Marine Science and Engineering Guangdong Laboratory (Zhanjiang), Zhanjiang 524000, China

Published online: 28 March 2024

$r_{re,G}$	Price of separating CO_2 from produced gas, \$/m^3
$r_{re,W}$	Processing cost of produced water, \$/m^3
s_i	Transformed model control variables
t	Index used for time
TAX_{CO2}	Incentive subsidy for CO_2 sequestration, \$/m^3
u^l_{opt}	Best control variable in the L iteration step
V_{CCS}	The amount of stored CO_2 volume, m^3
$V_{CO2}{}^i$	Cumulative gas injection volume, m^3

Greek letters

Δ^l	±1, Bernoulli distribution
α	Constant value, 0.602
η	Constant value, 0.101

Abbreviations

BHP	Bottom hole pressure
CCUS	Carbon capture, utilization and storage
EnOpt	Ensemble-based optimization
EnKF	Ensemble Kalman filter
EOR	Enhance oil recovery
FOPT	Field oil production total
GA	Genetic algorithm
GWO	Grey wolf optimizer
MMP	Minimum miscibility pressure
NEWUOA	New unconstrained optimization algorithm
NPV	Net present value
PSO	Particle swarm optimization algorithm
SA	Simulated annealing algorithm
SPSA	Simultaneous perturbation stochastic approximation
WAG	Water-alternating-gas
WSM	Weighted sum method

Introduction

After more than 40 years of water injection development, many oilfields in China have been seriously flooded and the remaining oil is always dispersed. It is more difficult for water injection to enhance oil recovery, although chemical flooding such as polymer flooding and surfactant flooding is introduced, reservoirs with high salinity are not suitable for chemical flooding. Therefore, it is vital to introduce innovative and efficient EOR methods. CO_2-EOR has been widely used since the 1980s (Faltinson and Gunter 2011; Han et al. 2016; Zhou et al. 2016). At the end of the twentieth century, various oilfields in China, such as ShengLi and Jiangsu oilfields, carried out pilot tests for CO_2 flooding. However, large-scale projects have not been implemented in China due to high cost and immature technology. Previous studies have demonstrated that CO_2 flooding can increase oil recovery by 10% to 20% after water flooding (Bagrezaie et al. 2014; Chen et al. 2016; Rezvani and Rafiei 2023). The mechanisms for CO_2-EOR in high-water cut reservoirs include: (1) In the process of CO_2 flooding, the wettability is changed, and the pore space originally occupied by oil or water is replaced by CO_2, which contributes to the migration of oil (Farahabadi and Lashkarbolooki 2023; Safaei-Farouji et al. 2022b). (2) CO_2 is easily dissolved in oil, and the mass transfer between oil and CO_2 reduces the difference of density between oil and gas phases, which enhances the flowing capacity of oil. (3) CO_2 can enter smaller pores, and displace oil droplets into larger pores (Hu et al. 2018; Lü et al. 2017).

Besides the CO_2 EOR, when the high-water cut reservoir is exploited with no economics, this reservoir becomes an ideal place for CO_2 sequestration, which has high environmental and economic benefits(Tapia et al. 2016). The primary goals of CO_2-EOR and CO_2 sequestration in oil reservoirs are to maximize oil production, *NPV*, and the amount of CO_2 sequestration. Therefore, the optimization of CO_2 injection in high-water cut oil reservoirs is a multi-objective optimization problem. A common way to solve this issue is the presentation of combined objective functions by introducing weight factors for each objective, which is named as the Weighted Sum Method (WSM) (Kovscek and Cakici 2005). In essence, the multi-objective problem is transformed into a single-objective problem(You et al. 2020a). These solutions are relatively simple and direct. However, the WSM has some drawbacks. First, the weight factor of WSM is difficult to set accurately, and the selection of the weight factor is blind. Additionally, WSM may result in an uneven distribution of solutions. To address these issues, the method of Pareto front is introduced by Coello et al. (2004), which is a repository that can provide multiple objectives with the same optimal level and can provide information on the trade-off between multiple objectives. It is more flexible than WSM in solving multiple objectives (Liu and Reynolds 2016). However, the acquirement of a set of Pareto fronts can be expensive computationally. Although the classical gradient solution method for single objective function is employed (Bender and Yilmaz 2014; Chen and Reynolds 2018), and the proxy models are constructed with machine learning (Liu et al. 2023; Safaei-Farouji et al. 2022a; You et al. 2020b), the calculation is also time-consuming.

In the previous studies for multi-objective functions, it was impossible to consider the cost of CO_2 injection and quantify the benefits of CO_2 sequestration. Thus, it is significant to present an optimal solution based on economic evaluation (Wang et al. 2018). Jahangiri and Zhang (2011) optimized the *NPV* under CO_2 miscible and immiscible flooding conditions by adjusting the wells' bottom-hole pressure. Leach et al. (2011) presented the function for collaborative optimization of oil recovery and

NPV. Rezvani and Rafiei (2023) optimized the *NPV* of CO_2 flooding through the Grey Wolf Optimizer (GWO) to delay the CO_2 breakthrough time. Chen et al. (2009a) proposed an objective function for averaging *NPV*, and a modified genetic algorithm (GA) is utilized as an optimization engine to determine the optimal production-injection strategy. However, these presented objective functions neglect the benefits of the application of recycling CO_2 recovered from producers. In addition, the optimization of production schemes is greatly emphasized, nevertheless, the optimal gas injection time for high-water cut reservoirs is often ignored by many researchers. Therefore, in this paper, the costs of capture, transport, and carbon subsidies are taken into account in the *NPV* function for CO_2 flooding in high-water-cut oil reservoirs. The benefits of recycling CO_2 for production wells correspond to the differences in costs for CO_2 injection and purification. Moreover, the *NPV* will be affected by the cost of CO_2 injection and the price of CO_2 subsidies. This paper investigates the optimal timing for switching from water flooding to CO_2 injection based on variations in injection cost and subsidies' price.

The optimization model for CO_2 EOR and sequestration in this paper is a typical nonlinear, nonconvex, no-smooth-constrained problem. Based on the discrete maximum principle, the adjoint method is an efficient approach for computing gradients in most optimization problems, this method has high efficiency, which can obtain accurate results. However, the implementation of the adjoint coding heavily relies on the source code of the reservoir simulator, which renders the solution process complex (De Montleau et al. 2006). Non-gradient algorithms do not require explicit gradient computations, which provides a potential solution to overcome the limitations of gradient-based methods. Generally, non-gradient algorithms can be categorized into three categories. The first is the heuristic random search algorithms, which include the simulated annealing algorithm (SA), GA, particle swarm optimization algorithm (PSO), etc. These algorithms are global search techniques, and can be capable of finding global optimal solutions but suffer from low computational efficiency (Kashkooli et al. 2022). The second category is to establish interpolation approximation models to replace original objective functions, which include the New Unconstrained Optimization Algorithm (NEWUOA) and the Wedge algorithm (Arenas et al. 2001; Emerick and Reynolds 2011; Zhang et al. 2015). However, for these algorithms, the construction of interpolation functions requires numerous simulations, which makes it difficult to satisfy the actual requirements. The third category is to obtain approximate gradients along the search directions, such as Ensemble-based Optimization (EnOpt) algorithm and Ensemble Kalman Filter (EnKF) method. The EnOpt algorithm has high computation capabilities, while the calculation direction may not always align with uphill directions to maintain stability. Although the EnKF method has good robustness, its convergence performance is mediocre(Chen et al. 2010, 2009b). In 2007, Gao et al. (2007) introduced the SPSA into the field for automatic history match, and found that the algorithm had a good fitting during the case tests. As SPSA is an approximate gradient algorithm, it eliminates the need for adjoint methods to compute gradients and is convenient for integration with various commercial simulators. The combination of this optimization method with simulators enables rapid calculation of optimal production variables. Therefore, in this paper, the SPSA is used indeed.

The paper is organized as follows: firstly, we establish an objective function based on *NPV*, which considers production and sequestration incomes. Then, with consideration of water cuts for different production periods, the CMG-GEM module is used to model the typical high-water cut reservoir. Thereafter, the SPSA algorithm with multiple perturbation averaging is applied, and the process of coupling with CMG-GEM is introduced in detail. Finally, the optimization results of gas injection to high-water cut reservoirs with different water cuts are analyzed, and the sensitivity of gas injection price and sequestration subsidy to the *NPV* are studied. In addition, the optimal production strategy for the WAG ratio is also determined.

Problem definition

For high-water cut oil reservoirs ($f_w > 60\%$), traditional water flooding can be replaced with CO_2 or WAG displacement for EOR. An objective function is presented to evaluate the reservoir's production efficiency, which includes some key indicators, such as oil production and CO_2 sequestration. During a fixed period, the production scheme is optimized based on the existing reservoir properties and fluid data. The following assumptions are made:

1. The investment of equipment and the depreciation of devices is ignored.
2. It is assumed that the price of CO_2 injection, the subsidy of sequestration, and the price of crude oil are constant.
3. Wells injection and production rates are limited by facilities.
4. The CO_2 from production wells is used for cyclic CO_2 injection.

According to the above assumptions, the optimal time of transferring from water flooding to CO_2 injection and the optimized CO_2 WAG ratio are determined in high-water cut oil reservoirs. In addition, it should be noted that the economic parameters, for example, the oil price, the costs of

gas and water injection, et al., are obtained from the average values of 2022.

Methodology

Model description

The project of injecting CO_2 into saline aquifers is unprofitable, while for CO_2-EOR in high-water cut reservoirs, the profits from oil production will offset the cost of CO_2 sequestration. The optimization of CO_2 sequestration and oil production in high-water cut oil reservoirs is the key to solving this problem and obtaining good benefits (Ampomah et al. 2017). Due to the high price of CO_2 gas sources, the traditional CO_2-EOR projects aim to reduce CO_2 injection and increase oil production as much as possible (Jahangiri and Zhang 2011, 2010; Kovscek and Cakici 2005), hence, the objective function can be expressed as Eq. (1).

$$f = \max(N_p) \cup \min(V^i_{CO_2}) \tag{1}$$

where N_p represents the cumulative oil production, and V^i_{CO2} represents the cumulative gas injection.

In this study, the maximum bottom hole pressure (*BHP*) for the injection well and the minimum *BHP* for the production well are determined appropriately. The production period is divided into different stages, and then the constraints for injection and production wells can be given separately for each time step. The boundary constraints are given as Eq. (2) and Eq. (3).

$$BHP^t_n \le BHP^{U,t}_n n \in \text{injector wells} \tag{2}$$

$$BHP^t_n \ge BHP^{L,t}_n n \in \text{producer wells} \tag{3}$$

where n is the number of perforated wells, t is time, and BHP^U is the upper boundary of *BHP*. BHP^L is the lower boundary of *BHP*. The rate of injection and production wells are taken as variables, and the upper and lower bounds for these variables are established (Tapia et al. 2016), which is shown in Eq. (4).

$$q^{L,t}_n \le q^t_n \le q^{U,t}_n n \in \text{injector wellsUproducer wells} \tag{4}$$

After the purification of the produced fluids, all of the produced CO_2 is used for cyclic injection, which is expressed as Eq. (5). The cost of CO_2 purification and cyclic injection is assumed to be constant.

$$q_{re} = \sum_n \sum_{t=0}^{T} q^t_{CO_2} \quad n \in \textit{producer wells} \tag{5}$$

In this paper, the amount of stored CO_2 in the high-water cut oil reservoir is determined by the differences between cumulative injected CO_2 and produced CO_2 volumes, which can be written as:

$$V_{CCS} = \sum_{t=0}^{T} \left(\sum Q^t_{g,i} - \sum Q^t_{g,p} \right) \tag{6}$$

The *NPV* is the discrepancy between the expected value of cash flow during the production process and the total investment, and the conventional form is expressed as Eq. (7).

$$NPV = \sum_{t=0}^{\mathrm{T}} \frac{C_t}{(1+r)^t} \tag{7}$$

where r is the discount rate, C_t is the cash flow at the time t, \$.

For water flooding in an oil reservoir, the equation of *NPV* is:

$$NPV = \sum_{t=0}^{T} \left(q^t_o r_o - q^t_{w,i} r_{w,i} - q^t_{w,p} r_{re,w} \right) / (1+r)^t \tag{8}$$

where q^t_{o} and r_{o} are the cumulative oil production rate at time t and the price of oil; $r_{\mathrm{w,i}}$ and $r_{\mathrm{re,w}}$ are the cost of water injection and the processing cost of produced water. $q^t_{\mathrm{w,i}}$ is the cumulative water injection rate at time t, and $q^t_{\mathrm{w,p}}$ is the cumulative water production rate at time t.

The subsidy of CO_2 sequestration is considered in the *NPV* function for the CO_2-EOR process. CO_2 sequestration in a saline aquifer or depleted reservoir is a non-profit project. However, for CO_2-EOR in high-water cut reservoirs, due to the consideration of subsidy income for CO_2 sequestration, these projects will have two sources of income. One is the benefit of oil production, and the other is the subsidy from CO_2 sequestration. With consideration of the above factors for CO_2-EOR in high-water cut reservoirs, the *NPV* objective function was presented as Eq. (9).

$$NPV = \sum_{t=0}^{T} \begin{matrix} (q^t_o r_o - q^t_{g,i} r_{g,i} - q^t_{w,i} r_{w,i} - q^t_{g,p} r_{re,g} + \\ q^t_{g,p} r_g - q^t_{w,p} r_{re,w} + V^t_{CCS} TAX_{CO_2}) \end{matrix} / (1+r)^t \tag{9}$$

This formula can be applied to continuous gas flooding and CO_2 WAG flooding. For continuous gas flooding, the $q^t_{\mathrm{w,i}}$ is ignored. $r_{\mathrm{g,i}}$ is the total cost of injected gas, which includes the costs of CO_2 capture, compression, transport, injection, and monitoring. It depends on the capture process, the volume of CO_2, the distance from the gas source to the injection wells, etc. $r_{\mathrm{re,g}}$ is the price of separating CO_2 from produced gas, and $q^t_{\mathrm{g,p}}$ is the volume of CO_2 separated from production wells, $q^t_{\mathrm{g,i}}$ is the cumulative volume of injected CO_2 during the production time. CO_2 stored tax

credit (TAX_{CO2}) is the subsidy for CO_2 sequestration from the government.

During the optimization for injection and production schemes, unrefined constraints on the upper and lower bounds of the model can impact the optimization outcomes (Guo and Reynolds 2018; Suykens et al. 2002). Therefore, it is necessary to address these constraints. For these boundary constraints, the logarithmic transformation method was used.

The formula of the logarithmic transformation method is listed as follows:

$$s_i = \ln \frac{m_i^U - m_i}{m_i - m_i^L} \tag{10}$$

where m_i is the optimization variable, s_i is the transformed optimization variable, m_i^L is the upper boundary of m_i, m_i^U is the lower boundary of m_i. With the logarithmic transform, boundary-constrained optimization can be transformed into an unconstrained optimization problem. When the iteration is completed, s_i is solved inversely.

Solution strategy

The problems of production optimization in reservoirs can be solved through the utilization of various approaches. The SPSA is employed to estimate the gradient since it overcomes the drawbacks of the conventional adjoint technique for solving gradients. Additionally, through the utilization of the projection gradient method and logarithmic transformation methods, a set of constraints for boundary conditions is dealt with judiciously. The algorithm is written in Fortran, and the CMG-GEM module is used to calculate the simulation results in parallel and iteratively. The flowchart for this optimization method is shown in Fig. 1. The data are transmitted and written between Fortran and CMG-GEM, the main function is composed of the presented *NPV* function, optimization algorithm, and CMG-GEM simulator. For this optimization process, firstly, the reservoir model for CO_2 flooding should be developed, and then the production and injection schemes are written into the file, which are seen as the main control variables. Secondly, the calculation results are simulated by CMG-GEM, and the objective function can be calculated after reading the calculation results. Thirdly, the SPSA generates the disturbance vector and calculates the disturbance gradient. Finally, the new control variables are calculated by random approximation, and the iteration process is repeated until the maximum number of iterations is attained.

The SPSA is a stochastic optimization method that employs an approximate steepest descent (or ascent)

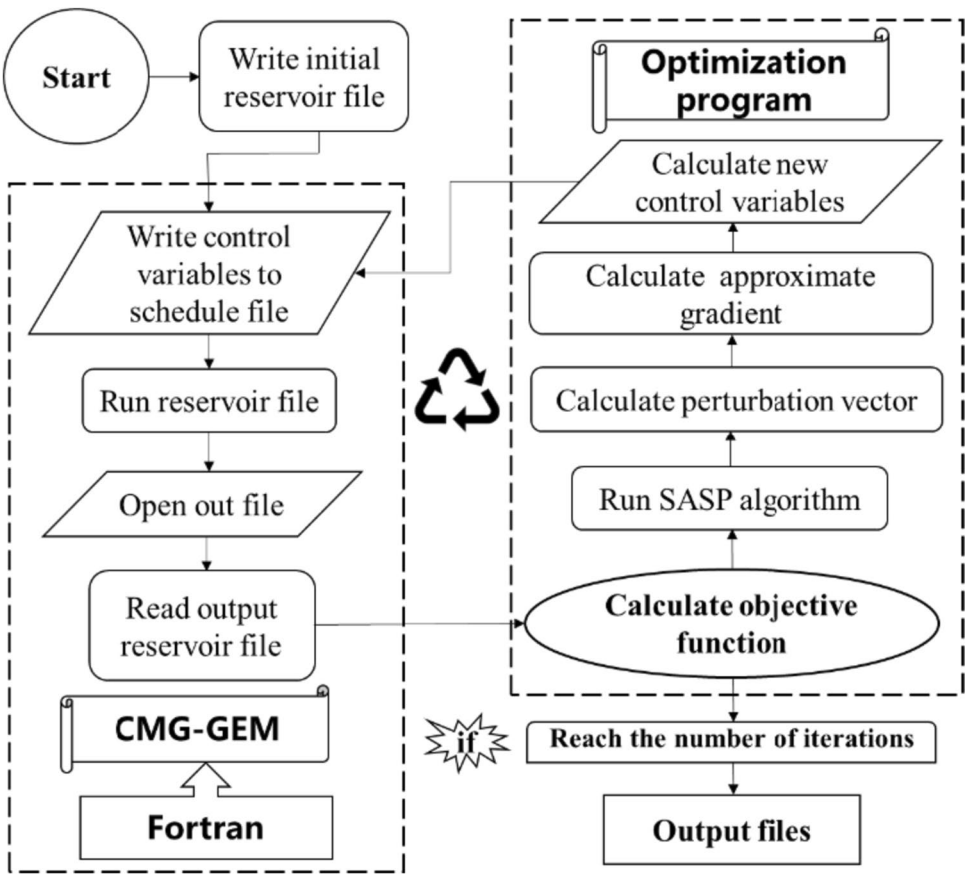

Fig. 1 The process of the optimization method

with a randomly selected stencil (Spall 2000, 1992). The algorithmic procedure of the SPSA algorithm is listed as follows:

(1) Initialization. The counter index k is set to be 1, and the production regimes and coefficients to produce the sequence $\{a_k\}$, $\{c_k\}$ are chosen, where $a_k = a/(A+k+1)^a$, $c_k = c/(k+1)^\eta$(a, c, A, α, η as parameters), $\alpha = 0.602$, $\eta = 0.101$;
(2) Generate simultaneous disturbance vectors. A P-dimensional random disturbance vector Δ is generated by the Monte Carlo rule, where each element in Δ is independent of each other, which follows the Bernoulli distribution;
(3) Estimate the objective function. Generate two measurements with a disturbance strategy in the objective function;
(4) Generate a gradient approximation. Generate a simultaneous perturbation approximation to the unknown gradient function;
(5) Update the estimates. Using the stochastic approximation form;
(6) Iteration or end. If the stop condition is not met, $k = k+1$, go to step 2; If the maximum number of iterations is attained, the iteration ends;
(7) Output the results.

In the L iteration step, the objective function is based on the simultaneous perturbation of all elements generated near the u^l_{opt}, which is shown in Eq. (11).

$$\hat{g}\left(u^l_{\text{opt}}\right) = \frac{J\left(u^l_{\text{opt}} + c_1\Delta^l\right) - J\left(u^l_{\text{opt}}\right)}{c_1\Delta^l_i} \tag{11}$$

where u^l_{opt} is the best control variable in the L iteration step. c_1 is the perturbation quantity, Δ^l is the value + 1 or −1, which conforms to the Bernoulli distribution.

However, in the production optimization on target reservoirs, due to the continuous optimization, there will be new search directions, and multiple gradients generated. To improve the accuracy of the algorithm, the average value of the gradient is used as the new search direction, and the disturbance gradient is averaged, as shown in Eq. (12).

$$\hat{g}^l\left(u^l_{opt}\right) = \frac{1}{M}\sum_{j=0}^{M}\hat{g}^l_j\left(u^l_{opt}\right) \tag{12}$$

where M is the sample size of the SPSA gradient. The iterative equation for the control variables is shown in Eq. (13).

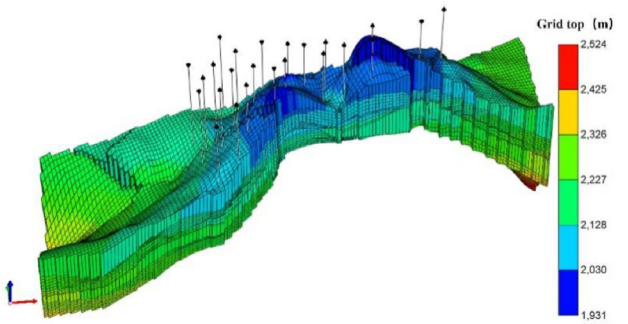

Fig. 2 A 3D view and Grid bottom of the reservoir

Table 1 Initial reservoir properties

Parameters	Value	Parameters	Value
Initial reservoir pressure/MPa	21.5	Average porosity	0.277
Reservoir temperature/℃	87	Number of planes	15
Oil viscosity/mPa·s	1.44	Current water cut	0.86
Water–Oil Contact/m	2260	Number of injectors	15
Average permeability/mD	250	Number of producers	9

$$u^{l+1}_{\text{opt}} = u^l_{\text{opt}} + a_l\hat{g}^l\left(u^l_{\text{opt}}\right) \tag{13}$$

where α_l is the step size in the search process.

Finally, the calculation is terminated when the difference of results between the contiguous two iterations is small, or when the maximum iteration step is reached. During the production period, various stages are involved. In CMG-GEM, the upper and lower limits of *BHP* are set, and then some optimization variables, such as injection and production rates, are determined under the constraints of *BHP*.

Case study

A 3D geological model is developed, which has 47 × 169 × 21 grid blocks in total. This model is depicted in Fig. 2. This reservoir is located in the Shengli oilfield, which is a complex fault block reservoir with medium porosity, high permeability, normal temperature, and pressure. The reservoir consists of numerous thin layers in the vertical direction, and exhibits significant heterogeneity. The detailed physical information for this reservoir is shown in Table 1. After decades of water flooding, the water cut in this block increased gradually. It is shown in Fig. 3 that the water saturation for more than half of the grids is higher than 0.7. Currently, the oilfield has a high-water cut of 86%. The reservoir contains 15 production wells and 9 injection wells,

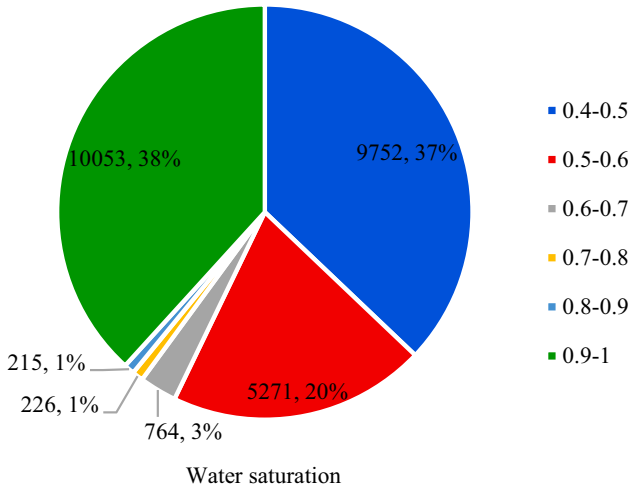

Fig. 3 The histogram of grid water saturation

Table 2 Composition of reservoir fluid

Components	Composition/%
N_2	0.3
CO_2	0.45
CH_4	24.4
C_2-C_4	8.3
C_5-C_9	25.73
C_{10}-C_{19}	30.86
C_{20}-C_{29}	9.9
C_{30+}	0.03

and has good connectivity between injection and production wells.

The composition of crude oil for this block is shown in Table 2, where the ratio of compositions for C_5 to C_{19} are relatively large, which causes that the Minimum Miscibility Pressure (MMP) is low (Elgaghah et al. 2007). The CMG-WINPROP module was used to fit the experimental data. The calculated MMP between oil and CO_2 is 24.5 MPa. The formation pressure in this field is close to 20–25 MPa due to the energy supply from water flooding. Therefore, the CO_2 flooding in this region is miscible or near-miscible displacement under the current formation pressure. The water–oil relative permeability curves and oil–gas relative permeability curves are obtained from laboratory experiments, which are shown in Fig. 4.

To compare with other schemes, multiple gas injection cases are designed reasonably, and the initial gas injection time is also investigated. The well injection and production rate are optimized, and the optimization period for gas injection is 30 months. The schedule of production and injection wells was changed every three months, which results in a total of 10 steps during the optimization process.

Results and discussion

Continuous gas injection

In the later stages of water flooding, oil production gradually decreases as water cut increases. The utilization of CO_2 flooding for EOR has the potential to yield significant benefits. However, it is crucial to determine the optimal timing for transitioning from water flooding to gas injection. Therefore, this study examines the impact of different switching times on the production performance of the reservoir. After a specific period of oil production and water injection, the reservoir formation pressure, as well as the oil and water saturation, will attain a certain status, which is served as the time point for gas flooding. This study presents five well-designed examples with production periods of 22, 23, 24, 27, 31, and 36 years, in which the water cuts for these production periods are 0.68, 0.75, 0.82, 0.86, 0.93, and 0.97, respectively. Table 3 shows the initial water saturation and pressure for the target oil reservoir. The upper and lower limits for the oil well production rate and water injection rate are given, which are obtained by multiplying the current

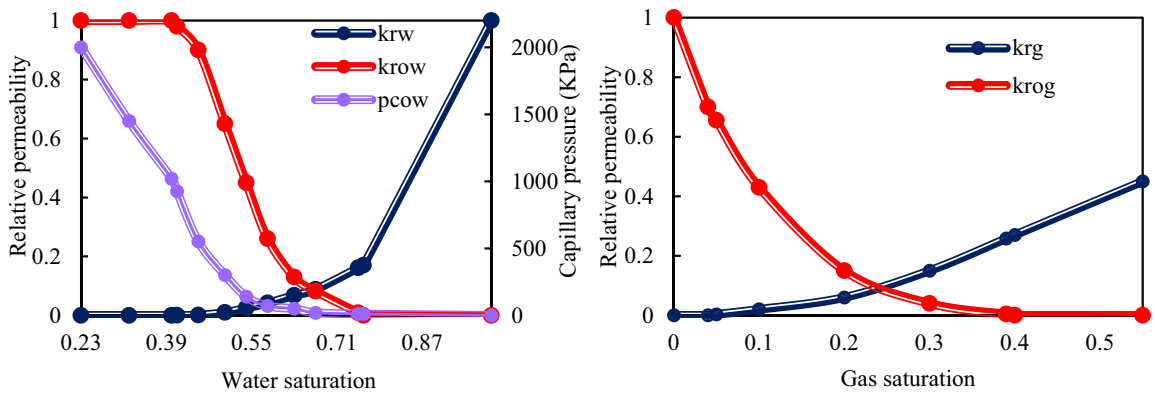

Fig. 4 Water–oil and gas-oil relative permeability curves

Table 3 A 3D view of reservoir water saturation and pressure

	Water saturation	Pressure
Water cut 0.68	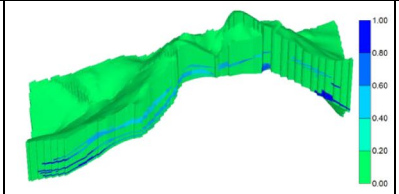	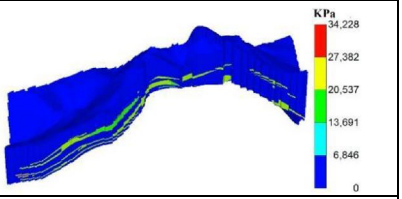
Water cut 0.75	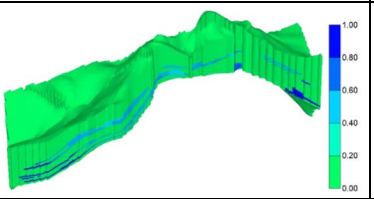	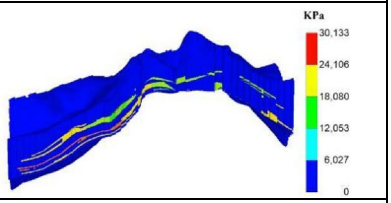
Water cut 0.82	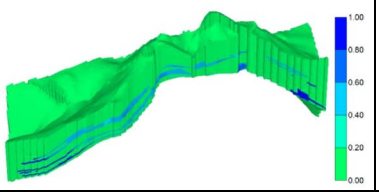	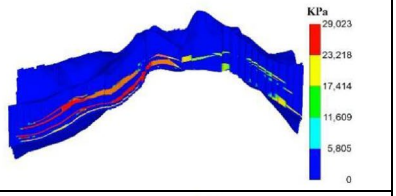
Water cut 0.86	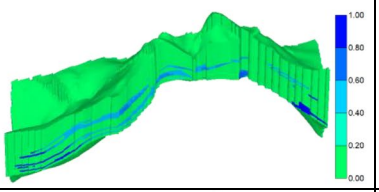	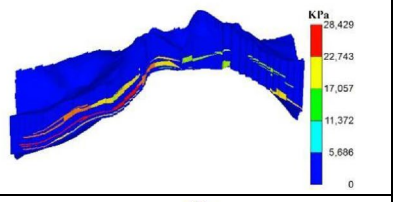
Water cut 0.93	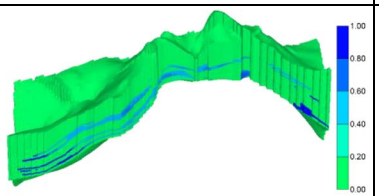	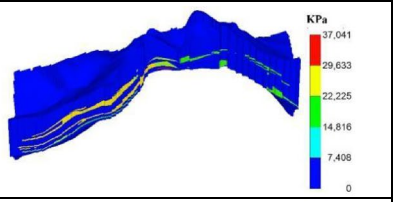
Water cut 0.97	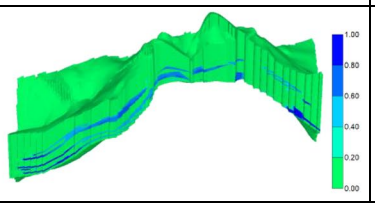	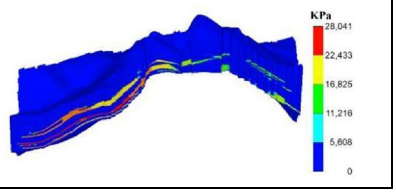

value by a coefficient. The variation coefficient for injection wells is 0–2, and for production wells, this coefficient is 0.5–2. The maximum injection pressure BHP^{U} is 50 MPa, and the production well BHP^{L} is 5 MPa. r_o is 564.96 \$/m^3, r_g is 0.097 \$/m^3, $r_{re,g}$ is 0.0223 \$/m^3, TAX_{CO2} is 0.0172 \$/m^3.

In the continuous gas injection process, the *NPV* function ignores the $q^t_{w,i}$. By using the SPSA algorithm, the optimized production scheme's *NPV* is obtained after 10 iterations. However, it is important to note that as the model runs, the remaining oil in the reservoir will decrease inevitably. Therefore, it is not sufficient to rely solely on the *NPV* to determine the timing of switching from water flooding to gas injection. Many factors, such as CO_2 breakthrough and cumulative oil production, should be also considered when the best injection timing is evaluated.

Production dynamics for different water cuts of switching gas injection are shown in Fig. 5. In Fig. 5a, it can be seen that the curves of cumulative oil production are close to linearity, and the earlier the gas injection time, the greater the cumulative oil production. As shown in Fig. 5b, no matter when CO_2 is injected, the water cut will rise slowly for about one hundred days and then decrease continually. It is also shown in Fig. 5c that the CO_2 sequestration capacity is the largest when the water cut is 0.68, and the CO_2 sequestration capacity at different injection times is similar. In Fig. 5d, it can be found that the CO_2 breakthrough time for the periods with different water cuts is basically between 200 and 300 days, and the final production of CO_2 is relatively close. It is worth noting that for the case of water cut 0.86, compared to other cases, the breakthrough of CO_2

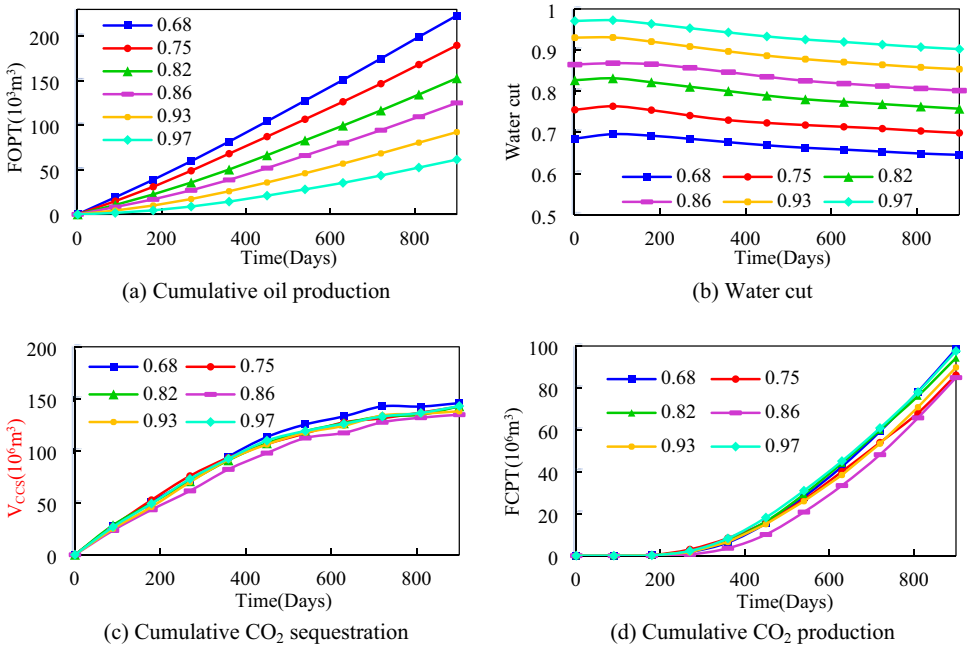

(a) Cumulative oil production (b) Water cut

(c) Cumulative CO_2 sequestration (d) Cumulative CO_2 production

Fig. 5 Production dynamics after CO_2 injection for oil reservoir with different water cut

is the latest, and as the water cut increased, the time of CO_2 breakthrough decreased rapidly. The reason why the CO_2 breakthrough time for water cut 0.86 is the longest is that the optimized CO_2 injection rate is lower than the other cases, which can be found in Fig. 5c (before the CO_2 breakthrough, the sequestration volume is equal to the injection volume). After the CO_2 breakthrough, the injection rate is also lower than the other cases, as shown in Fig. 5c, d (after the CO_2 breakthrough, the total injection volume is equal to the sum of sequestration and production volume). In other cases, the injection rate does not change greatly, hence, the CO_2 breakthrough time increases with the water cut. It indicates that the water saturation will affect the flow of CO_2 in the high-water cut reservoir, which can reduce the contact area between oil and CO_2, and thus affect the breakthrough of injected CO_2.

To reflect the differences in production dynamics between CO_2 and water flooding, the discrepancies in cumulative oil production rate and water cut at the end of production time for these two cases are shown in Fig. 6. It is shown in Fig. 6a that compared with water injection, gas injection yields higher cumulative oil production, and the crude oil produced by gas injection in the early stage is much larger than water injection, but the amount of crude oil production decreases rapidly when the water cut is equal to 0.93. Figure 6b illustrates the reduction of water cuts after CO_2 flooding at the end for cases with different initial water cuts. When the water cut is 0.93, the reduction is the highest. The figure also demonstrates how the water cut will affect the seepage of oil, gas, and water. When the water cut is higher, the reduction of the water cut is larger after gas flooding. However, it should be noted that the merits of traditional water flooding are low injection costs and high safety. The comparison of *NPV* between gas injection and water injection is shown in Fig. 7. The *NPV* of gas injection and water injection will decrease with the rise of production time, but the decline rate of the *NPV* for gas injection

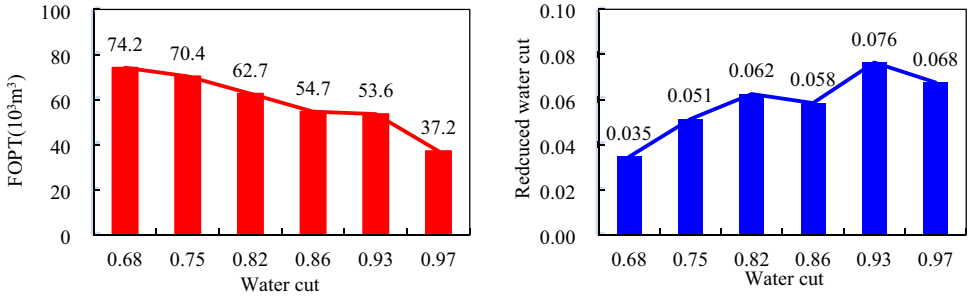

(a) Final reduction of cumulative oil production (b) Final reduction of water cut

Fig. 6 Comparison of production dynamics between water injection and CO_2 injection for reservoirs with different water cut

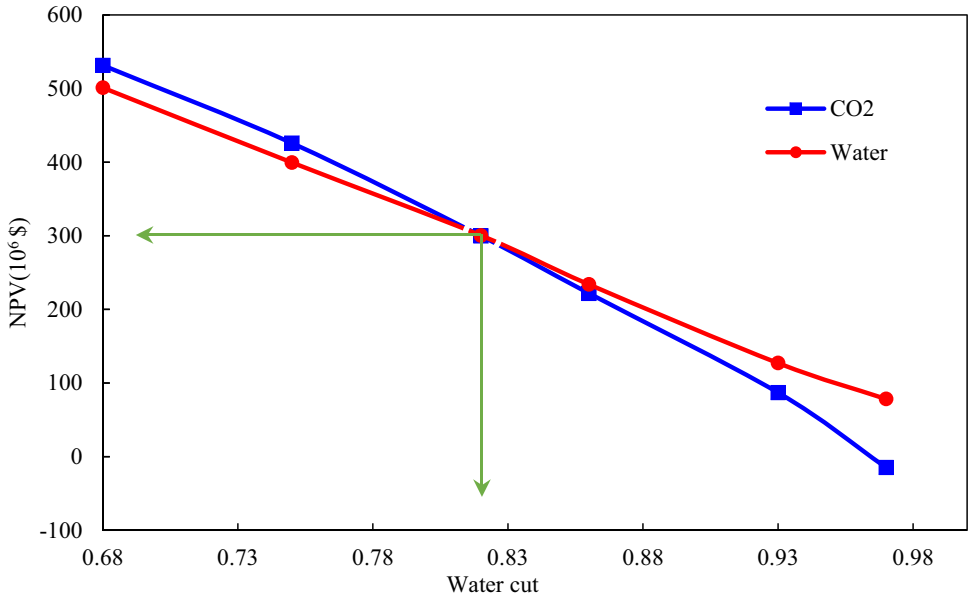

Fig. 7 *NPV* for water injection and gas injection under different water cut

production is significantly higher than the development of water injection. When the water cut is 0.68, the *NPV* of gas injection is higher than that of water injection. Nevertheless, when the water cut is larger than 0.82, the *NPV* of the water injection exceeds the gas injection. When the water cut reaches 0.97, the water injection approach is still profitable, while gas injection becomes non-profitable. After linear regression of the *NPV* curve, we found that when the water cut is 0.82, the benefits of water injection and gas injection intersect, which indicates that the timing of gas injection should be earlier than the period with a water cut of 0.82.

Sensitivity of injection cost

To study the sensitivity of *NPV* to the price of injected gas, scenarios with different CO_2 injection costs were set, and the *NPV* for these scenarios was compared. When the price of CO_2 injection varies in a reasonable range (0.119–0.238), the variation of *NPV* is also very sensitive. It can be seen that the price of gas injection has a great influence on the economic benefits of gas injection development. As shown in Fig. 8, as the price of injected gas rises, the economic benefit of CO_2 flooding is lower than water flooding, and the intersect time is getting earlier. However, the variation in gas injection prices will not change the trend that water injection is more economical than gas injection in the later stages. After linear

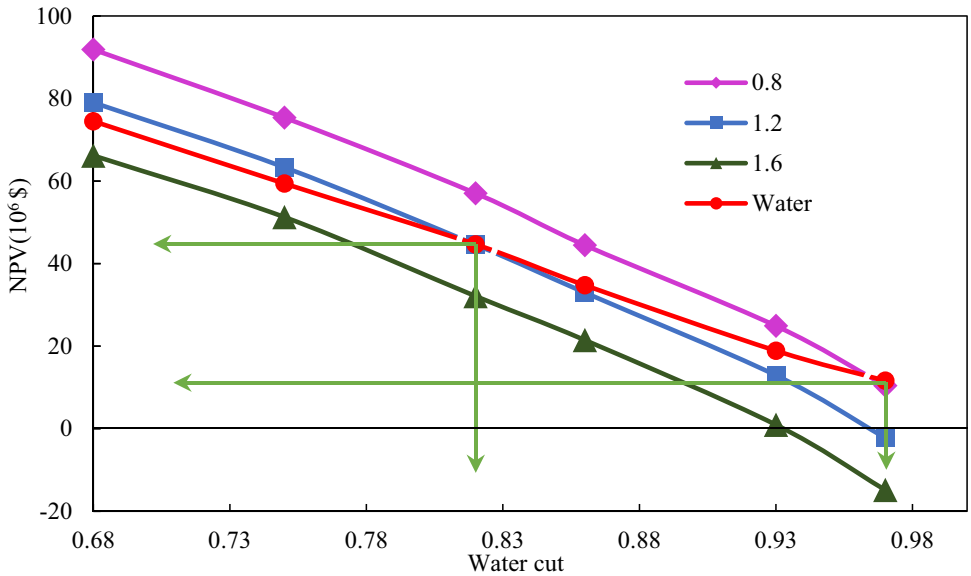

Fig. 8 *NPV* of different gas injection cost

regression, the results indicate that the gas injection cost is 0.119 $/m^3 and the water injection has a crossing point with the water cut of 0.97. This shows that when the gas injection price is 0.119 $/m^3, as long as the water cut is less than 0.97, the gas injection is more profitable than water flooding. When the injection price is 0.238 $/m^3 and the water cut is larger than 0.93, the economic benefit of gas injection is lower than that of water injection. While the injection price is 0.178 $/m^3, it should be switched to gas injection to maintain profitability before the water cut is less than 0.97.

Sensitivity of TAX_{CO2} income

Besides the price of gas injection, the TAX_{CO2} revenue from government subsidies may also have significant impacts on the *NPV*. With the reservoir water cut increasing, the *NPV* obtained from production gradually declined, but the economic benefits brought by CO_2 storage remain unchanged, hence, the benefits brought by CO_2 sequestration in the later stage were more critical. Therefore, the prices of different subsidies are set, and the influences of different TAX_{CO2} on *NPV* for reservoirs with different water cuts are shown in Fig. 9. With the water cut increase, the decreasing trend of *NPV* remains unchanged. Furthermore, the increase of sequestration subsidies within a reasonable range has minimal effect on *NPV*, however, the profits from CO_2 sequestration in different periods are relatively consistent.

With the CO_2 subsidy price increasing, the economic benefit of CO_2 sequestration is higher, and the time when the benefit of water flooding is higher than CO_2 flooding (or the corresponding water cut in injection time) is later. When the sequestration subsidy is 0.0169 $/m^3, CO_2 flooding is more profitable than water flooding before the water cut is lower than 0.82. When the sequestration subsidy increases to 0.0297 $/m^3, CO_2 flooding is better than water flooding when the water cut is 0.86 or less. When the sequestration subsidy is 0.0743 $/m^3, CO_2 flooding yields a higher *NPV* than water flooding when the water cut is 0.93 or less. When the sequestration subsidy is less than 0.0743 $/m^3, CO_2 flooding will be unprofitable when the water cut is 0.97. However, when the subsidy reaches 0.0743 $/m^3, even if the water cut is higher than 0.97, CO_2 flooding remains profitable due to the high sequestration benefits. Even when the subsidy reaches 0.0743 $ /m^3, water flooding still yields more *NPV* than CO_2 flooding.

WAG injection

Due to the lower viscosity and density of CO_2, compared with water flooding, viscous fingering, and gravity override usually occur during CO_2 flooding, which can lead to poor CO_2 sweep efficiency. By alternately injecting CO_2 and water, it can reduce the relative permeability of gas, and effectively lower the mobility of injected fluids, which can weaken the gas viscous fingering effect, delay CO_2 breakthrough time, and improve the swept efficiency. This measure is named WAG flooding. The WAG ratio is defined as the ratio of water and gas injection slugs. In practice, the WAG ratios are set to be 1:1, 1:2, and 2:1.

To compare the results of different schemes, with the presented model, calculations are conducted. As shown in Fig. 10a, it can be found that the *NPV* for the WAG ratio 1:2 and 1:1 is better than other cases. The initial *NPV* for the WAG ratio 2:1 is better, but in the later stage, the growth rate of income begins to decline. Finally, it is almost the same as a continuous

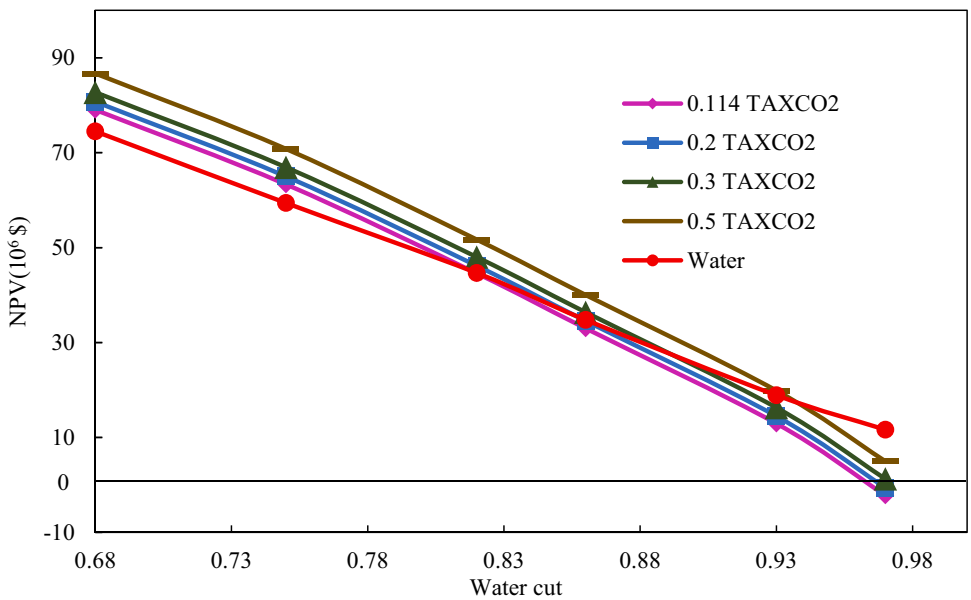

Fig. 9 *NPV* for different TAX_{CO2}

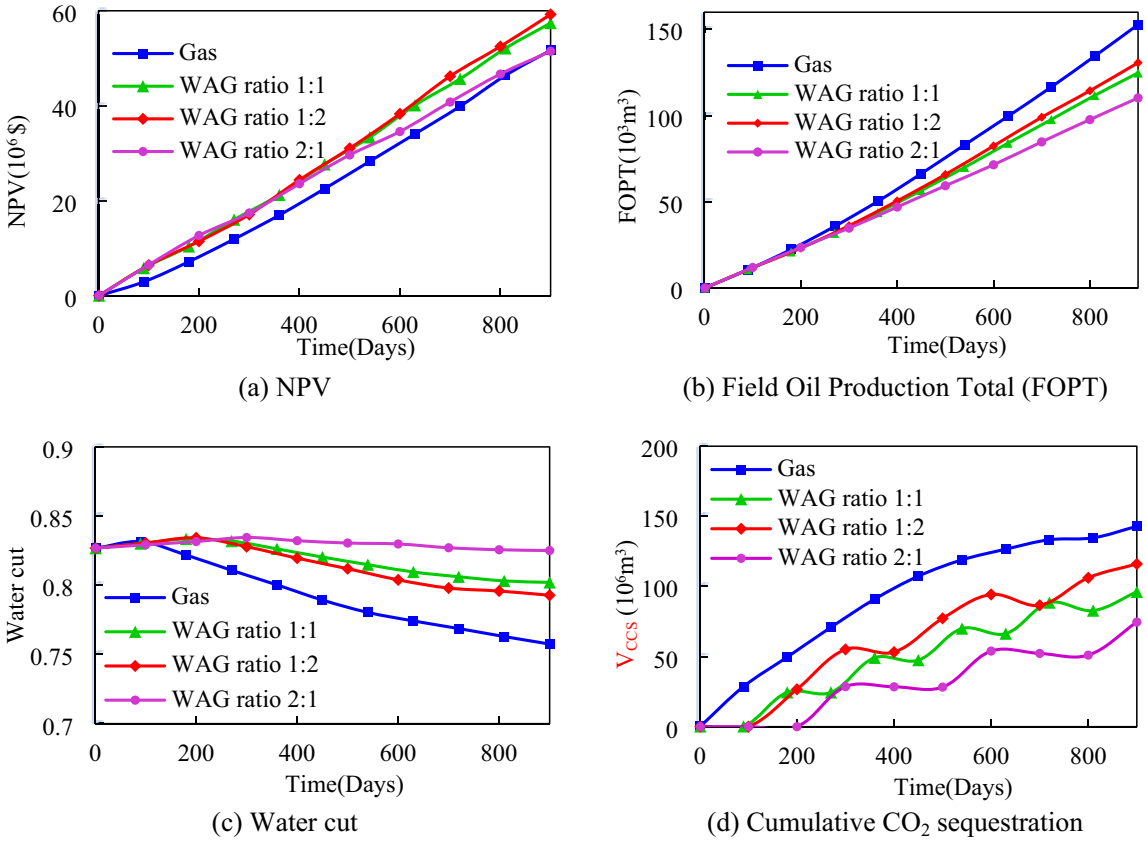

Fig. 10 Production dynamics after WAG injection for oil reservoir with different WAG ratio

gas injection. As shown in Fig. 10b, for a WAG ratio 2:1, it is hard to displace the remaining oil in the later stage due to the low gas injection volume, therefore, the field cumulative oil production declines rapidly in the middle stage, which is the reason for the decrease of *NPV*. As shown in Fig. 10b, c, when the WAG ratio increases, the cumulative oil production rate decreases, and the increase in the water–gas ratio will result in a smaller reduction in the water cut. When the WAG ratio is 2:1, the water cut in the production period remains almost unchanged. This shows that the higher the gas ratio in the production period, the more oil is displaced, and the more water cut is reduced. From Fig. 10d, it can be seen that the sequestration of continuous gas injection is the largest, however, continuous gas injection also results in the earliest gas breakthrough. The WAG curve in Fig. 10d exhibits fluctuating trends since CO_2 is produced during the water injection. Through the comprehensive evaluation of the *NPV*, field cumulative oil production, water cut, and CO_2 sequestration, the scheme with WAG ratio 1:2 is the best.

Conclusions

In this paper, for the issue of collaborative optimization for CO_2 flooding EOR and sequestration in high-water cut oil reservoirs, an optimization methodology for this issue is presented. Through the combination of an efficient algorithm and CMG-GEM numerical simulation module, the optimal CO_2 injection time and WAG ratio are determined. The sensitivity of injection cost and TAX_{CO2} income to *NPV* is analyzed. The following conclusions could be drawn:

(1) A novel objective function that considers the economic parameters of oil production and CO_2 sequestration is established for CO_2 flooding in high-water cut oil reservoirs, which is solved with the efficient SPSA algorithm coupling with the CMG-GEM module.
(2) In the high-water cut stage, the earlier the gas injection time, the higher the economic benefits obtained. When the water cut reaches 0.97, the gas injection development will be non-profitable, while water injection is still profitable.

(3) The variation of gas injection cost to *NPV* is more sensitive than the change in carbon sequestration subsidy. When the gas injection price is 0.238 \$/m^3, CO_2 flooding is more profitable than water injection development at any time. When the water cut is 0.97, the carbon sequestration subsidy income is greater than the oil production income, therefore, to promote Carbon Capture, Utilization and Storage (CCUS), the government should increase the subsidy for the CO_2 flooding in high-water cut oil fields.

(4) The cumulative oil production rate for gas injection is higher than WAG flooding, but the *NPV* for gas injection is lower than WAG flooding. The large WAG ratio (2:1) has poor benefits in high-water cut reservoirs.

Acknowledgements This work was supported by the National Natural Science Foundation of China (Grant No. 52104018), and CNPC Science and Technology Major Project (Grant No. 2021DJ1504). The authors would like to appreciate reviewers and editors whose critical comments were helpful in preparing this article.

Funding Fund was provided by National Natural Science Foundation of China (Grant No.: 52104018), CNPC Science and Technology Major Project (Grant No.: 2021DJ1504).

Declarations

Conflict of interest The authors declare no potential conflicts of interest with respect to the research, author- ship, or publication of this article.

Data availability The data that support the findings of this study will be available from the corresponding author upon request.

References

Ampomah W, Balch RS, Grigg RB, McPherson B, Will RA, Lee SY (2017) Co-optimization of CO_2-EOR and storage processes in mature oil reservoirs. Greenhouse Gases Sci Technol 7(1):128–142. https://doi.org/10.1002/ghg.1618

Bagrezaie M A, Pourafshary P, Gerami S (2014) Study of different water alternating carbon dioxide injection methods in various injection patterns in an Iranian non fractured carbonate reservoir. in: Offshore Technol Conf-Asia. https://doi.org/10.4043/24793-ms

Bender S, Yilmaz M(2014) Full-field simulation and optimization study of mature IWAG injection in a heavy oil carbonate reservoir. in: SPE Improved Oil Recovery Symposium. https://doi.org/10.2118/169117-MS

Chen B, Reynolds AC (2018) CO_2 water-alternating-gas injection for enhanced oil recovery: optimal well controls and half-cycle lengths. Comput Chem Eng 113:44–56. https://doi.org/10.1016/j.compchemeng.2018.03.006

Chen Y, Oliver DS, Zhang D (2009b) Efficient ensemble-based closed-loop production optimization. SPE J 14(04):634–645. https://doi.org/10.2118/112873-PA

Chen C, Wang Y, Li G, Reynolds AC (2010) Closed-loop reservoir management on the Brugge test case. Comput Geosci 14:691–703. https://doi.org/10.1007/s10596-010-9181-7

Chen S, Li H, Yang D(2009a) Production optimization and uncertainty assessment in a CO_2 flooding reservoir. in: SPE Production and Operations Symposium. https://doi.org/10.2118/120642-MS

Chen H, Yang S, Liu J, Zhang X, Mei Y, Li X, Li Y(2016) Experimental study on injection strategy of CO_2 Near-miscible flooding in low permeability reservoirs with high water cut. in: International Petroleum Technology Conference. https://doi.org/10.2523/iptc-18770-ms

Coello CA, Pulido GT, Lechuga MS (2004) Handling multiple objectives with particle swarm optimization. IEEE Trans Evol Comput 8(3):256–279. https://doi.org/10.1109/TEVC.2004.826067

Elgaghah S, Zekri A, Almehaideb R, Shedid S(2007) Laboratory investigation of influences of initial oil saturation and oil viscosity on oil recovery by CO_2 miscible flooding. in: EUROPEC/EAGE Conference and Exhibition. https://doi.org/10.2118/106958-MS

Faltinson JR, Gunter B (2011) Net CO_2 stored in north American EOR projects. J Can Pet Technol. https://doi.org/10.2118/137730-PA

Farahabadi ZT, Lashkarbolooki M (2023) Effect of CO_2 on the interfacial tension and swelling of crude oil during carbonated water flooding. J Pet Explor Prod Technol 13(1):353–364. https://doi.org/10.1007/s13202-022-01554-6

Gao G, Li G, Reynolds AC (2007) A stochastic optimization algorithm for automatic history matching. SPE J 12(02):196–208. https://doi.org/10.2118/90065-PA

Guo Z, Reynolds AC (2018) Robust life-cycle production optimization with a support-vector-regression proxy. SPE J 23(06):2409–2427. https://doi.org/10.2118/191378-PA

Han J, Lee M, Lee W, Lee Y, Sung W (2016) Effect of gravity segregation on CO_2 sequestration and oil production during CO_2 flooding. Appl Energy 161:85–91. https://doi.org/10.1016/j.apenergy.2015.10.021

Hu W, Lü C, Rui W, Maolei C, Yang Y, Xin W (2018) Porous flow mechanisms and mass transfer characteristics of CO_2 miscible flooding after water flooding. Acta Petrolei Sinica 39(02):201–207. https://doi.org/10.7623/syxb201802008

Jahangiri HR, Zhang D (2010) Optimization of carbon dioxide sequestration and enhanced Oil recovery in oil reservoir. in: SPE Western Regional Meeting. https://doi.org/10.2118/133594-MS

Jahangiri HR, Zhang D (2011) Optimization of the net present value of carbon dioxide sequestration and enhanced oil recovery. in: Offshore Technology Conference. https://doi.org/10.4043/21985-MS

Kashkooli SB, Gandomkar A, Riazi M, Tavallali MS (2022) Coupled optimization of carbon dioxide sequestration and CO_2 enhanced oil recovery. J Petrol Sci Eng 208:109257. https://doi.org/10.1016/j.petrol.2021.109257

Kovscek AR, Cakici MD (2005) Geologic storage of carbon dioxide and enhanced oil recovery. II. Cooptimization of storage and recovery. Energy Convers. Manage. 46(11–12):1941–1956. https://doi.org/10.1016/j.enconman.2004.09.009

Leach A, Mason CF, Veld KVT (2011) Co-optimization of enhanced oil recovery and carbon sequestration. Resour Energy Econ. https://doi.org/10.1016/j.reseneeco.2010.11.002

Liu M, Fu X, Meng L, Du X, Zhang X, Zhang Y (2023) Prediction of CO_2 storage performance in reservoirs based on optimized neural networks. Geoenergy Sci Eng 211428. https://doi.org/10.1016/j.geoen.2023.211428

Liu X, Reynolds AC (2016) Gradient-based multiobjective optimization for maximizing expectation and minimizing uncertainty or risk with application to optimal well-control problem with only bound constraints. SPE J 21(05):1813–1829. https://doi.org/10.2118/173216-PA

Lü C, Wang R, Cui M, Yongqiang T, Xia Z (2017) Displacement experiment of CO_2 miscible flooding under high water condition. Acta Petrolei Sinica 38(11):1293. https://doi.org/10.7623/syxb201711008

De Montleau P, Cominelli A, Neylon K, Rowan D, Pallister I, Tesaker O, Nygard I(2006) Production optimization under constraints using adjoint gradients. in: ECMOR X-10th European Conference on the Mathematics of Oil Recovery. https://doi.org/10.3997/2214-4609.201402506

Rezvani H, Rafiei Y (2023) A novel analytical technique for determining inflow control devices flow area in CO_2-EOR and CCUS projects. J. Pet. Explor. Prod. Technol. 1–12. https://doi.org/10.1007/s13202-023-01654-x

Safaei-Farouji M, Thanh HV, Dai Z, Mehbodniya A, Rahimi M, Ashraf U, Radwan AE (2022a) Exploring the power of machine learning to predict carbon dioxide trapping efficiency in saline aquifers for carbon geological storage project. J Cleaner Prod 372:133778. https://doi.org/10.1016/j.jclepro.2022.133778

Safaei-Farouji M, Thanh HV, Dashtgoli DS, Yasin Q, Radwan AE, Ashraf U, Lee K-K (2022b) Application of robust intelligent schemes for accurate modelling interfacial tension of CO_2 brine systems: Implications for structural CO_2 trapping. Fuel 319:123821. https://doi.org/10.1016/j.fuel.2022.123821

Spall JC (1992) Multivariate stochastic approximation using a simultaneous perturbation gradient approximation. IEEE Trans Autom Control 37(3):332–341. https://doi.org/10.1109/9.119632

Spall JC (2000) Adaptive stochastic approximation by the simultaneous perturbation method. IEEE Trans Autom Control 45(10):1839–1853. https://doi.org/10.1109/TAC.2000.880982

Suykens JA, De Brabanter J, Lukas L, Vandewalle J (2002) Weighted least squares support vector machines: robustness and sparse approximation. Neurocomputing 48(1–4):85–105. https://doi.org/10.1016/S0925-2312(01)00644-0

Tapia JFD, Lee J-Y, Ooi REH, Foo DCY, Tan RR (2016) Optimal CO_2 allocation and scheduling in enhanced oil recovery (EOR) operations. Appl Energy 184:337–345. https://doi.org/10.1016/j.apenergy.2016.09.093

Wang X, van't Veld K, Marcy P, Huzurbazar S, Alvarado V (2018) Economic co-optimization of oil recovery and CO_2 sequestration. Appl Energy 222:132–147. https://doi.org/10.1016/j.apenergy.2018.03.166

You J, Ampomah W, Sun Q, Kutsienyo EJ, Balch RS, Dai Z, Cather M, Zhang X (2020b) Machine learning based co-optimization of carbon dioxide sequestration and oil recovery in CO_2-EOR project. J Cleaner Prod 260:120866. https://doi.org/10.1016/j.jclepro.2020.120866

You J, Ampomah W, Sun Q (2020a) Co-optimizing water-alternating-carbon dioxide injection projects using a machine learning assisted computational framework. Appl Energy 279. https://doi.org/10.1016/j.apenergy.2020.115695

Zhou Y, Wang R, Gou F, Lang D (2016) CO_2 flooding mechanism in high water cut reservoirs. Acta Petrolei Sinica 37(S1):143–150. https://doi.org/10.7623/syxb2016S1014